LA-UR- 97-2018

Approved for public release; distribution is unlimited.

Title: NONINVASIVE MEASUREMENT OF ACOUSTIC PROPERTIES OF FLUIDS USING ULTRASONIC INTERFEROMETRY TECHNIQUE

Author(s): Wei Han, Dipen N. Sinha, Kendall N. Springer and David C. Lizon

Submitted to: 8th International Symposium on Non Destructive Characterization of Materials, Boulder, CO June 15 - 20, 1997

Los Alamos
NATIONAL LABORATORY

DISCLAIMER

NONINVASIVE MEASUREMENT OF ACOUSTIC PROPERTIES OF FLUIDS USING ULTRASONIC INTERFEROMETRY TECHNIQUE

W. Han, D.N. Sinha, K. N. Springer and D. C. Lizon

Electronic and Electrochemical Materials & Devices Group, MS D429
Los Alamos National Laboratory
Los Alamos, NM 87545

Abstract – A swept-frequency ultrasonic interferometry technique is used for noninvasively determining acoustic properties of fluids inside containers. Measurements over a frequency range 1-15 MHz on six liquid chemicals are presented. Measurements were made with the liquid inside standard rectangular optical glass cells and stainless steel cylindrical shells. A theoretical model based on one-dimensional planar acoustic wave propagation through multi-layered media is employed for the interpretation of the observed resonance (interference) spectrum. Two analytical methods, derived from the transmission model are used for determination of sound speed, sound attenuation coefficient, and density of liquids from the relative amplitude and half-power peak width of the observed resonance peaks. Effects of the container material and geometrical properties, path-length, wall thickness are also studied. This study shows that the interferometry technique and the experimental method developed are capable of accurate determination of sound speed, sound attenuation, and density in fluids completely noninvasively. It is a capable and versatile fluid characterization technique and has many potential NDE applications.

INTRODUCTION

Sound propagation studies have been used for many years to extract information about the physicochemical properties of fluids such as liquids, solutions, suspensions and emulsions. Measurements of ultrasonic attenuation and speed as a function of frequency provide an excellent tool for the investigation of chemical relaxation in liquids and for the characterization of suspensions and emulsions in terms of particle size and concentration. At low frequencies (below 1 MHz), sound speed and attenuation measurements have typically used the resonance reverberation techniques[1-3]. This requires a large volume of liquid. High-frequency (1-100 MHz) measurements typically use the swept frequency ultrasonic interferomery technique developed several decades ago [4-7]. Even higher frequency measurements can be made using the pulse-echo technique [8, 9]. An excellent comprehensive review of the various techniques has been provided by Eggers and Kaatze [4]. The ultrasonic interferometry technique is generally considered to be an excellent method because of its high precision and its ability to work with small liquid samples[5, 7]. For many industrial and environmental monitoring processes, especially those involving toxic and hazardous chemicals, it is desirable to have the capability to noninvasively determine physical properties of the liquid contents in various containers. Traditional ultrasonic interferometry technique mentioned above requires the transducers to be in direct contact with the fluid being tested, thus restricting the use of this technique to highly specialized laboratory characterization of fluids. Sinha et al.[10] recently extended the capability of the

traditional ultrasonic interferometry technique by adapting it for noninvasive measurements in identifying chemical warfare compounds inside sealed chemical munitions.

In this paper, we specifically address noninvasive ultrasonic interferometry technique and theory, and present results of measurements on acoustic properties (sound speed, attenuation and density) in fluids inside a container. The fluids tested include six liquid chemicals in standard rectangular optical glass cells and a cylindrical steel shell. Effects of the container geometrical parameters, such as path-length and container shape were studied. We show how accurate determination of both sound speed and attenuation in liquids over a frequency range (1-15 MHz) can be made inside ordinary containers without using custom-designed finely machined resonator cells. A theoretical model based on normal acoustic wave propagation through multiple-layered media[11] is used to explain the various features observed in the spectra and to derive two analytical methods for extraction of sound attenuation and liquid density from the measured resonance spectrum. One method is based on frequency-dependent relative strengths of minima and maxima (peak) of the spectrum, and the other is based on half-power bandwidth of the resonance. The good agreement of the measured physical parameters with literature values illustrates the potential of the interfrometry technique for noninvasive characterization of fluids in industrial applications as well as in basic research.

THEORETICAL ANALYSIS

Theoretical analysis for determining acoustic properties in fluids noninvasively is presented based on the acoustic transmission and reflection through multiple-layered media, which consists of transducer, wear plate, coupling gel layer, cell wall and specimen fluid inside the cell. The multiple-layer model formulation is analogous to the well-known theory of planar wave propagation through one layer[12], and detailed description and solutions are given elsewhere [11]. By solving for transmitted and reflected pressure amplitudes in each layer in terms of outgoing transmitted wave amplitude, one gets the pressure transmission coefficient

$$\tilde{T} = \frac{2}{(1+z_1/z_2)\,\tilde{C}_{11} + (1-z_1/z_2)\,\tilde{C}_{12}} \tag{1}$$

z_1 and z_2 are specific impedance (ρc) for transducer and wear plate. The intensity transmission coefficient is a real quantity and given as

$$T_I = \left|\tilde{T}\right|^2 \tag{2}$$

which is amplitude of transmitted wave relative to the incident wave, and is what the experiment measures. $\tilde{C}_{11}$ and $\tilde{C}_{12}$ given elsewhere[11], are complicated functions of acoustic impedance, longitudinal speed and thickness of each medium, and of attenuation of fluid specimen. Eq. (2) shows intensity transmission spectrum contains information for extracting attenuation coefficient, wave speed, acoustic impedance of fluid. To derive an explicit, inverse solution for acoustic properties in fluid, one considers the simplified case[(zz)] of acoustic wave transmission through a fluid layer with pathlengh L and attenuation coefficient α_L, contained between two similar wall boundaries. As $\alpha_L L << 1$, the intensity transmission coefficient becomes [12]

$$T_I = \frac{1}{(1+\frac{1}{2}\sigma\,\alpha_L L)^2 + \frac{\sigma^2-4}{4} Sin^2 \frac{\omega}{c_L} L} \tag{3}$$

Here impedance ratio $\sigma = z_W/z_L + z_L/z_W$. For weakly loaded fluid inside an elastic cell, $\sigma \approx z_W/z_L$.

T_I in (3) is a periodic function of $\alpha_L L$ and σ, with minima $T_{I,\min} \approx \left(1+\frac{1}{2}\sigma\,\alpha_L L\right)^{-2} + \frac{\sigma^2-4}{4}$, at $f_n = (n+\frac{1}{2})\frac{c_L}{2L}$, and maxima $T_{I,\max} \approx \left(1+\frac{1}{2}\sigma\,\alpha_L L\right)^{-2}$, at $f_n = n\frac{c_L}{2L}$. Using the maxima and minima (peaks) of transmission spectra *separately* to determine the attenuation and the impedance of fluid-loaded plates has been reported by Guiddarelli et al[13], who used a similar one-layer transmission model approach, and by Fiorito et al [14], who employed a "resonance theory formalism" approach. Here, rearranging the mimima to maxima of transmission coefficient, one obtains

$$\left[\frac{1}{(T_{I,\min}/T_{I,\max})}-1\right]^{-0.5}=\frac{2}{\sigma}+\alpha L \tag{4}$$

Therefore, from the slope and intercept of linear fitting of $[(T_{min}/T_{max})^{-1} - 1]^{-0.5}$ vs. f^2 over the resonance frequency range, $\alpha_L L$ and σ can be determined.

Another traditional method is to determine the fluid attenuation coefficient from the half-power bandwidth of measured spectrum. Unlike the complexity of Eq.(2), from the intensity transmission coefficient Eq.(3), one can derive an inverse solution for half-power bandwidth δf in terms of acoustic properties in fluid [11]

$$\delta f=\frac{2\,c_L}{\pi\,\sigma\,L}+\frac{c_L\,\alpha_L}{\pi} \tag{5}$$

The second term is the well-known fluid attenuation and is identical to the solution of the ideal resonator theory [4, 5, 15], which was derived based on a finely-tuned transducer resonator cell that was in direct contact with the testing liquid. The first term $\delta f_0=\frac{2\,c_L}{\pi\,\sigma\,L}$ is independent of frequency and α_L and depends on σ, c_L and L. It is mainly resulted from the transmission and reflection energy loss at wall-liquid interface and therefore, can be used to infer acoustic and geometrical properties of both wall and fluid inside.

In practice, diffraction loss and instrumental loss also contributes to the half-power bandwidth and thus need to be properly corrected. In this study, measured δf is corrected for the diffraction using the expression of Labhardt and Schwarz [6], $\delta f_{diff}=\frac{0.147}{\pi\beta}\left(\frac{2\,c_L}{D}\right)^3 f^{-2}$. Here D is the effective diameter of transducer element and $\beta = z_L/z_W$. Instrumental loss including transducer backing loss, transducer misalignment and viscous boundary loss at the wall-liquid interface, can be calibrated with a standard liquid of known acoustic properties [4, 5, 6, 15]. Thus, attenuation coefficient of testing liquid α_L is

$$\alpha_L=\frac{\pi}{c_L}(\delta f-\delta f_0)-\frac{\pi}{c_L}(\delta f_r-\delta f_{r0})+\frac{c_r}{c_L}\alpha_r \tag{6}$$

δf and δf_r are measured half-power bandwidth, for testing and reference liquids. δf_0 and δf_{r0} are extrapolated width as $f^2 \to 0$, for test and reference fluids. c_r and α_r are sound speed and attenuation coefficient of reference liquid. From the slopes $(\delta f-\delta f_0)/f^2$ and $(\delta f_r-\delta f_{r0})/f^2$, attenuation coefficient factor $\alpha_0=(\alpha_L/f^2)10^{17}$ (np s^2 / cm) can be measured. From δf_0, density of testing fluid can be determined with the noting that $\sigma \approx \rho_W c_W / \rho_L c_L$

$$\rho_L=\delta f_0\frac{\pi\,c_w\,\rho_w\,L}{2\,c_L^{\,2}} \tag{7}$$

From the liquid resonance frequency difference $\Delta f = f_{n+1} - f_n$ and L, sound speed in fluid can be measured independently by $c_L = 2\,\Delta f\,L$. However, experiments and model predictions [11] found that Δf varies within 1% of mean values, due to effects of wall resonance modulation. c_L is thus obtained using average of peak-peak distances $<\Delta f>$ over each fluid frequency resonance segment

$$c=2\,L\,<\Delta f> \tag{8}$$

EXPERIMENTAL SETUP

The ultrasonic interferometer depicted in Fig. 1, consists of five sections; a rectangular cell containing a liquid to be tested, a Digital Synthesizer and Analyzer (NEEL Electronics, CA) computer plug-in-card, two disk-shaped piezoelectric transducers, a PC computer and a voltage amplifier. The DSA board contains all electronics for sweep signal generation and signal processing circuitry for analyzing the detected signal. The sweep frequency range available is 1 KHz - 15 MHz. The sweep time can be varied from 800 frequency steps per second to 1 step per second. With a frequency resolution of 0.1 Hz over the entire frequency range, the system provides a frequency response directly in real-time. Typical excitation voltage level is

approximately 1 v or less. The broad-band lithium niobate transducers (Panametrics Corp., MA) with resonance frequency of 5 - 10 MHz are used. The system operates as follows. A sine-wave voltage excitation that is gradually increasing in frequency in time, is generated by the RF signal generator of the DSA board. The electric signal is applied to the input transducer, which converts the sine-wave voltage signal to sound waves that propagates through the cell container wall and the liquid inside. A second identical transducer used as a receiver is parallelly attached to the opposite side of the cell and detects the outgoing signal after it propagates through the container wall and the fluid. The received signals are amplified by an voltage amplifier having 34/54 dB gain. The detecting unit of the DSA board measures the amplitude and the phase (for homodyne mode) of the voltage signal as a function of sweeping frequency. The measured amplitude spectrum is digitized and is analyzed by a FORTRAN code, which searches for position and half-band width for each resonance peak and determines sound speed, attenuation and density of testing liquid using the theoretical model described above. Two kinds of container are tested, optically polished rectangular glass cell (Starna Cells, Inc., CA, longitudinal speed c_W =5640 m/s and ρ = 2.558 g/cm^3) and cylindrical stainless steel shell with inner diameter 5.27 cm (c_W =5790 m/s, ρ = 7.9 g/cm^3). In the measurement, several important factors can affect the consistency and accuracy of results of the acoustic parameters. These include careful adjustment of transducer alignment, proper use of liquid gel to maintain uniform coupling, accurate temperature control, and proper selection of frequency range.

RESULTS AND DISCUSSION

The principle of operation of acoustic interferometry is the setting up the standing waves in a resonator cavity using external excitation and simultaneously detection. For measurement made from the excitation of transducer attached outside of a cell container, the resulting interference spectrum is a superimposition of both the interference pattern in the liquid itself and that in the wall, as shown in Fig. 2(a), where measurement was made for isopropanol in optical glass cell. As shown in the Fig. 2(b), the predicted normalized transmission spectrum using the multi-layered model Eq. (2) has good agreement with the measurement data. The liquid peaks are sharp with smaller periodicity than the wall peaks that are separate farther apart. The respective peak separation is mainly depended on the pathlength in the liquid and the thickness of the wall in additional to the sound speeds in both media. The main wall harmonic resonance peaks occur at about 5 and 7 MHz, where the liquid peaks becomes broadening and the peak-peak distances narrows, due to the stronger wall resonance modulation effect. Around 4, 6, and 8 MHz, the spectrum is the interference pattern in the fluid, where the peak widths are mainly influenced by the acoustic impedance mismatch between the liquid and wall material δf_0, as well as by the sound absorption in the liquid and the instrumental loss. The position, height and width of liquid resonance, are weakly influenced by the wall resonance modulation. The two analytical solutions Eqs.(4) and (5)are primarily applicable in those frequency ranges where the resonance peaks are selected for analysis.

As shown in Eq (21), the first part of the half-band width derived from the one-layer transmission model is frequency-independent impedance mismatch contribution. It is the sound energy loss due to the multiple reflection and transmission at wall-liquid boundary, and is inversely proportional to the pathlength L and acoustic impedance ratio z_w/z_L. Fig. 3 shows the measured half-power width on glycerin in three rectangular glass cells of 2, 5 and 10 mm in pathlength at 28.4 °C. The measurement are in reasonably good agreement with predictions obtained using Eq. (5). The average liquid attenuation coefficient factor $\alpha_0 = (\alpha_L / f^2)10^{17}$ ≈ 1530 nps^2/cm, is less sensitive to the changes in the cell pathlength L.

Although the theoretical model discussed applies to planar-shaped container, present technique can be easily adapted to measurement on circular cylindrical-shaped cavity, as illustrated in Fig. 4 In comparison with measurements on a rectangular planar-surfaced glass cell (L =1.0 cm), measured δf on a stainless steel cylinder (inner diameter L = 5.27 cm) filled with ethylene glycol are plotted vs. f^2. A curve-surfaced plastic pad, with one end being planar and other end having the same curvature as the cylinder cell, is used between the transducer and the cylindrical container. Besides providing the good surface contact, planar-concave intermediate layer focus the beam and thus reduces the diffraction loss [15]. The slope that determines the attenuation of ethylene glycol is almost same. The uncalibrated attenuation coefficients factor α_0 are 246 and 254 (nps^2/cm) for both measurements. The different intercepts reflect the fact the two containers have different z_W/z_L. For the steel cell, the measured width shifted a constant value and is lower than that of the glass cell, suggesting the lower sound transmission and reflection loss at the wall-liquid boundary. This example shows the capability of interferometry technique in attenuation measurement regardless of the container geometry (planar or cylindrical) and material.

To illustrate the accurate measurement of sound speed of fluids, Fig. 5 shows the measured sound speed on six liquids glycerin, ethylene glycol, water, toluene, benzene and isopropanol in glass cell over f = 1-11

MHz. The average values of $<c_L>$ are 1887.38±10.49, 1668.01±6.51, 1487.58±8.81, 1286.62±3.6, 1275.77±2.95 and 1133.13±4.59 (m/s), for the above liquids. The maximum relative standard deviation in sound speed is 0.59%. The scattering of the sound speed is primarily due to the oscillations of Δf, as a result of the cell wall resonance modulation effects.

Half-power width δf are shown in Fig. 6 for glycerin, ethylene glycol, toluene, benzene and isopropanol at 26.8 °C. Toluene is selected as reference liquid for calibration of the optical glass cell. Also shown are the predicted half-power bandwidth using Eq. (5). The measured α_0 using Eq.(6) for glycerin, benzene, ethylene glycol and isopropanol are 1530, 778, 191.4 and 406, compared to the reported values[16] at 20 °C of 1500 (Bhatia[17], page 170), 860, 130 and 270. Relative errors in measured attenuation coefficients in comparison with the reported values are appreciably larger for the low attenuating isopropanol and ethylene glycol than for the higher attenuating benzene and glycerin, evidently due to the increase in relative contribution of instrumental loss. Other possible reasons include the variations in reported attenuation coefficient values and the lack of accurate temperature calibration of the measurement cell. It is evident that resolution for measurement of high-attenuation liquid is better than the low attenuating liquids.

The measured liquid density determined by Eq(7) is plotted in Fig. 7 along with the reported values for the testing liquids. The relative error for the five liquids is about ± (2 - 9) % , with maximum error occurred with isopropanol. Glycerin and ethylene glycol have lower relative error of +6.8% and −8.8%. Results on liquid density, based on the frequency-dependent half-power bandwidth measurement, are surprisingly in good agreement with the reported values.

We also tested capability of the interferometer and the method using relative strength of resonance peaks for attenuation and density measurements. In Fig. 8, values of $[(T_{min}/T_{max})^{-1} - 1]^{-0.5}$ are plotted vs. f^2, for benzene, ethylene glycol, isopropanol and toluene in glass cell (1 cm). As predicted by the theory, the data shows strong linearity of plot $[(T_{min}/T_{max})^{-1} - 1]^{-0.5}$ vs. f^2 over the frequency range considered. The measured attenuation coefficient factors α_0, determined from the slopes of linear fitting are 1380, 133, 294 and 67.5 for benzene, ethylene glycol, isopropanol and toluene, respectively. Except for higher measured attenuation for benzene, the agreements of the measured α_0 with the reported values (130, 270 and 82) are in general very good and are better than the half-width method. If use toluene as reference liquid, values of liquid density determined from the calibrated intercepts are 0.918, 1.068 and 0.566 g/cm^3, in good agreement with the reported values[16] of 0.88, 1.108 and 0.79 g/cm^3 for benzene, ethylene glycol and isopropanol.

CONCLUSION

It has been shown that the interferometry technique and theory developed here are capable of noninvasively measuring sound speed, attenuation coefficient and density in liquids contained in rectangular and cylindrical containers. The interferometer is a capable and versatile fluid characterization technique. The general theoretical model for the one-dimensional wave propagation through multiple-layered media provides good agreement with measurements. Two analytical methods developed yield good results in the measurement of acoustic properties in fluids. The swept-frequency ultrasonic interferometry has a wide range of applications, especially in the fields of evaluations of material properties and industrial process control.

ACKNOWLEDGMENT

This work was supported by the Office of the Assistant to the secretary of Defense, Counterproliferation program and by the Defense Special Weapons Agency.

REFERENCES

1. L. E. Lawley and R. D. Reed, "A reverberation method for the measurement of the absorption of ultrasonics in liquids", Acustica, **5**, 316-322 (1955).
2. V. S. Kononenko, "Precision method for measurement of the ultrasound absorption coefficient in liquids at frequencies of 0.1-20 MHz", Sov. Phys. Acoust., **33**, 401-404 (1987).
3. von P. Hauptmann, I. Alig and R. Säuberlich, "Statistical reverberation method for ultrasonic measurement in liquid polymeric systems", Acustica, **50**, 189-193 (1982).
4. F. Eggers and U. Kaatze, "Broad-band ultrasonic measurement techniques for liquids", Meas. Sci. Technol., **7**, 1-19 (1996).

5. F. Egger and Th. Funck, " Ultrasonic measurements with milliliter liquid samples in the 0.5- 100 MHz range", Rev. Sci. Instrum., **44**, 969-977 (1973).
6. A. Labhardt and G. Schwarz, "A high resolution and low volume ultrasonic resonator method for fast chemical relaxation measurements", Ber. Bunsenges. Phys. Chem., **80**, 83-92 (1976).
7. K. W. Katahara, C. S. Rai, M. H. Manghnani and J. Baloph, "An interferometric technique for measuring velocity and attenuation in molten rocks", J. Geophys. Res., **86**, 11779-11786 (1981).
8. W. Sachse and C. Chian, " Determination of the size and mechanical properties of a cylindrical fluid inclusion in an elastic solid", Material Evaluation, **33**(4), 81-85 (1975).
9. D.J. McClements and P. Fairley , "Frequency scanning ultrasonic pulse echo reflectometer", Ultrasonics, **30**, 403-405 (1992).
10. D. N. Sinha, B. W. Anthony and D. C. Lizon, "Sweep frequency acoustic interferometry technique for chemical weapons verification and monitoring", Third Intl. Conference On-Site Analysis, (1995).
11. W. Han, D.N. Sinha, K.N. Springer and D.C. Lizon, "An ultrasonic interferometry method for non invasive determiantion of acoustic properties in liquids", J. Acoust. Soc. Am., (in review).
12. L.E. Kinsler, A.R. Frey, A.B. Coppens and J.V. Sanders, *Fundamentals of Acoustics*, Chapter 6, Third Edition, John Wiley & Son (1982).
13. G. Guiddarelli, A. Mrini and L. Palmieri, "Ultrasonic method for determining attenuation coefficients in plate-shaped materials", J. Acoust. Soc. Am., **94**, 1476-141481 (1993).
14. R. Fiorito, W. Madigosky and H. Überall, "Acoustic resonances and the determination of the material parameters of a viscous fluid layer", J. Acoust. Soc. Am., **69**, 897-903(1981).
15. R. Brehends, F. Eggers, U. Kaatze and T. Telgmann, "Ultrasonic spectrometry of liquids below 1 MHz. Biconcave resonator cell with adjustable radius of curvature", Ultrasonics, **34**, 59- 67 (1996).
16. L.W. Anson and R.C. Chiver, "Thermal effects in the attenuation of ultrasound in dilute suspensions for low values of acoustic radius", Ultrasonics, **28**, 16-26 (1990).
17. A.B. Bhatia, *Ultrasonic Absorption*, , p170 & p260, Dover Publishing, Inc., NY (1967).

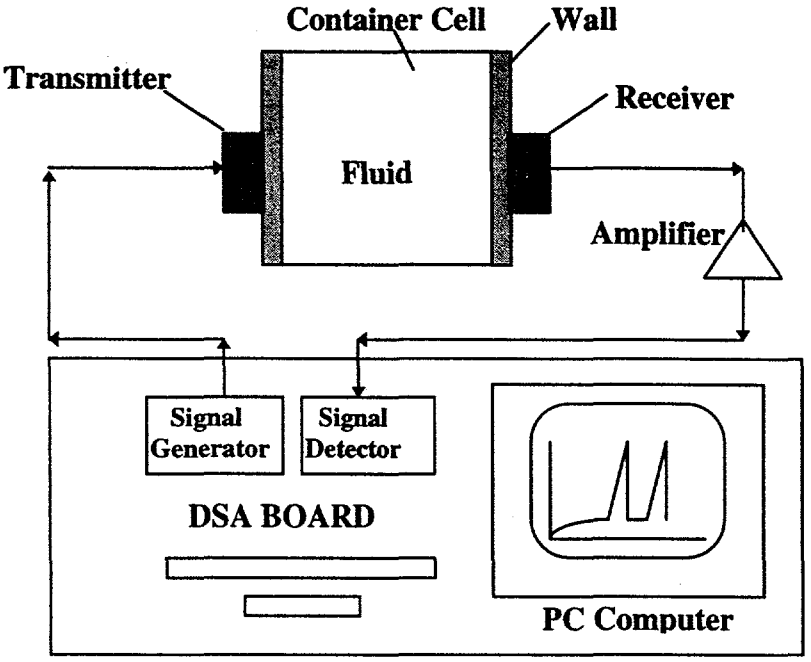

FIG. 1. Experimental set up of a swept-frequency ultrasonic interferometer

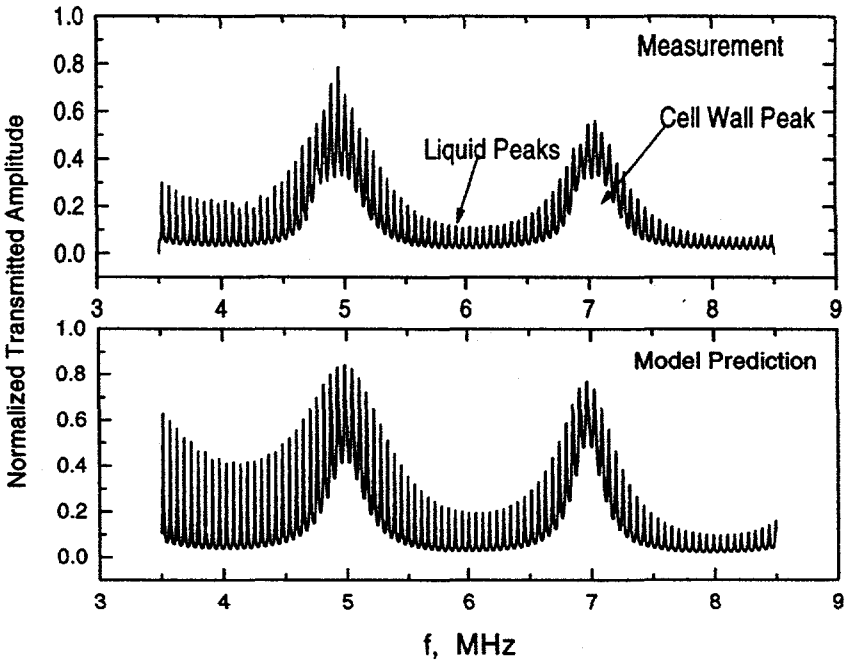

FIG. 2. Comparison of measured interference resonance spectrum with model prediction of Eq.(2) for isopropanol in glass cell (L =1.0 cm)

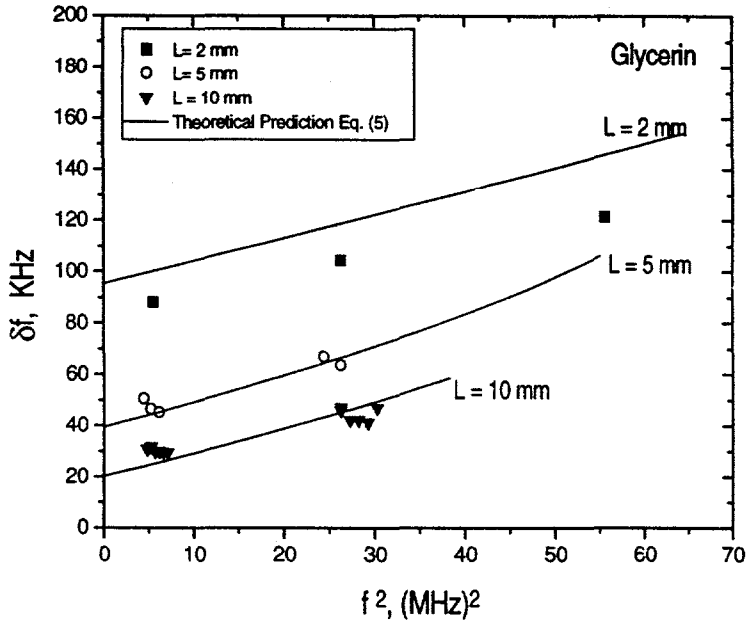

FIG. 3. Effect of liquid pathlength L on the half-power band width for glycerin in three glass cells of $L = 2.0$, 5.0 and 10.0 mm. T = 28.9 °C. Solid curves are predictions using Eq. (5).

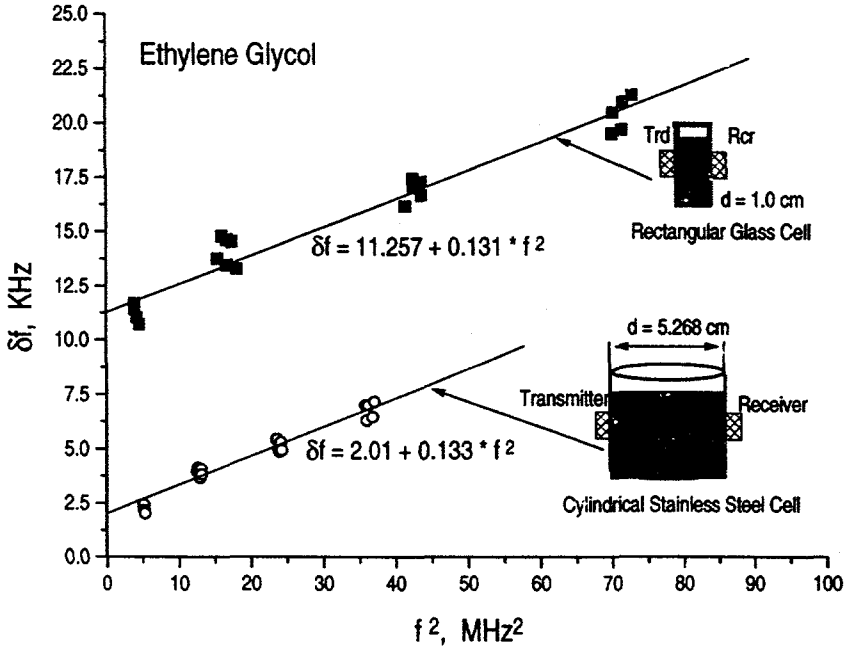

FIG. 4. Swept-frequency interferometry measurements on a planar glass cell (L=1 cm) and cylindrical stainless steel shell (L =5.27 cm) filled with ethylene glycol.

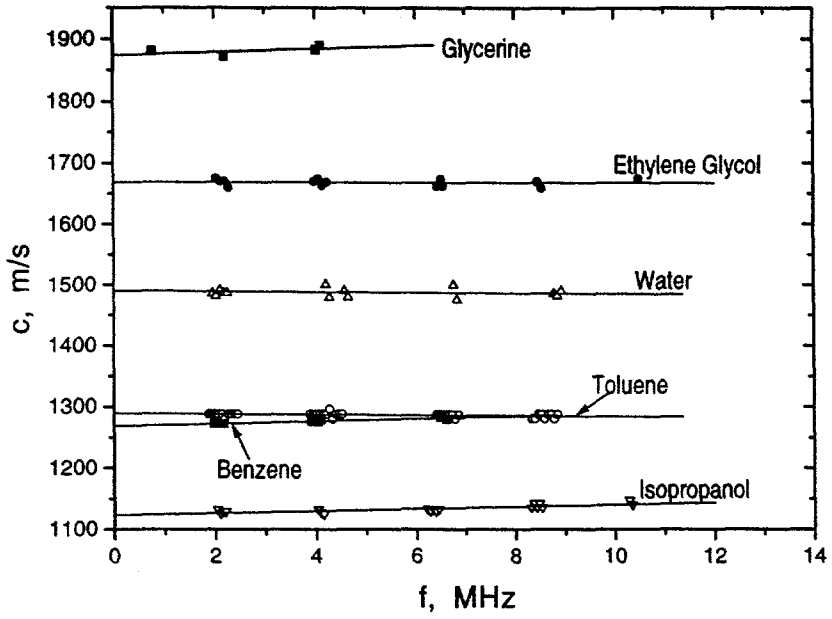

FIG. 5. Interferometry measurements on speed of sound in glycerin, ethylene glycol, water, toluene, benzene and isopropanol. $T = 24.0$ °C for water. $T = 26.8$ °C for other liquids.

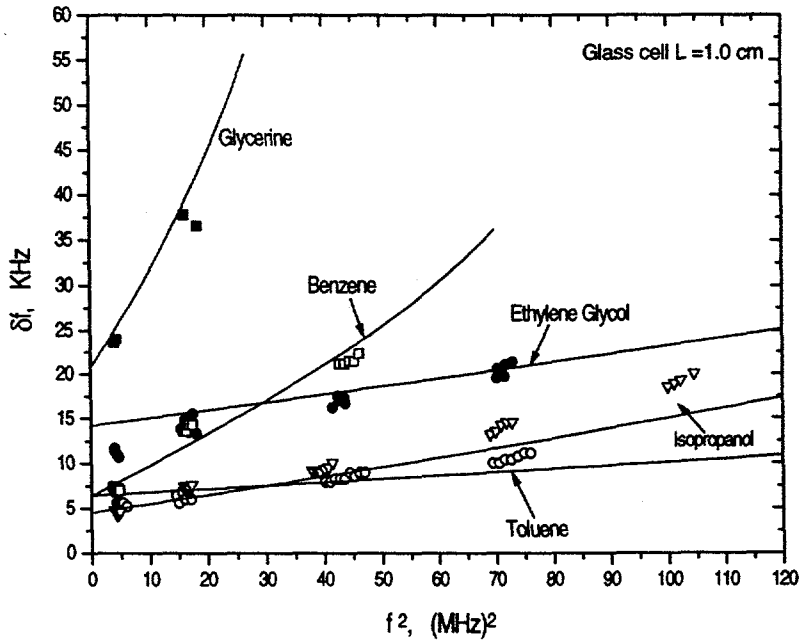

FIG. 6. Comparison of measured half-power bandwidth δf vs. f^2 with predictions for glycerin, benzene, ethylene glycol, isopropanol and toluene. Calibrated attenuation factor α_0=1530, 778, 191.4 and 406 np s^2/cm for the former four liquids.

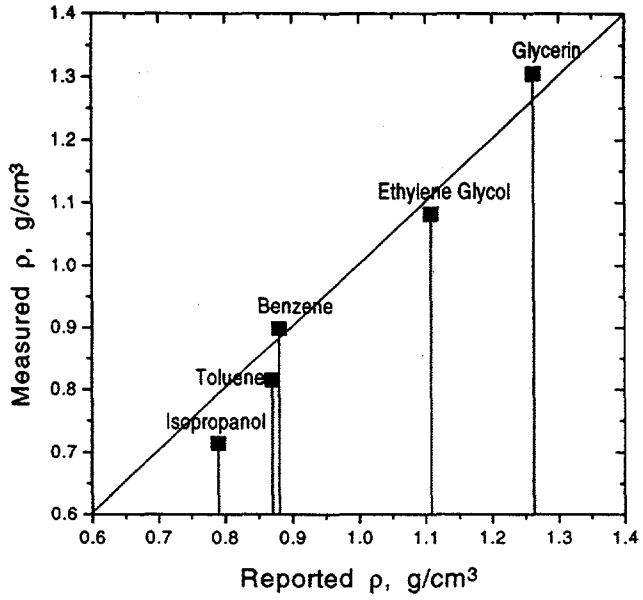

FIG. 7. Interferometry measurement on density of the five liquids in rectangular glass cell (L =1.0 cm) based on the half-power bandwidth approach

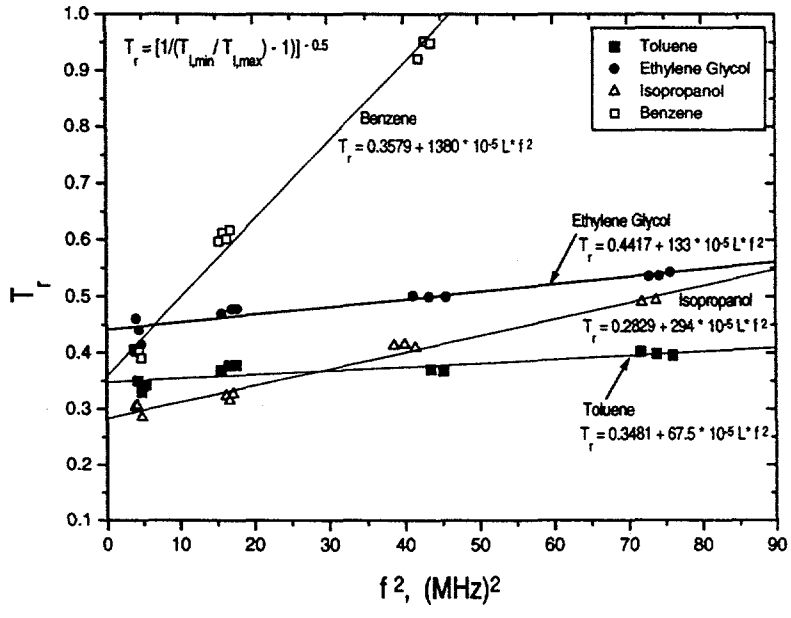

FIG. 8. Interferometry measurement on attenuation coefficient for four liquids in rectangular glass cell (L = 1.0 cm) based on the relative transmission strength approach.